Interannual stability of organic to inorganic carbon production on a coral atoll

Lester Kwiatkowski[1], Rebecca Albright[1], Jessica Hosfelt[2,3], Yana Nebuchina[1], Aaron Ninokawa[2,4], Tanya Rivlin[5,6], Marine Sesboüé[1], Kennedy Wolfe[7], and Ken Caldeira[1]

[1]Department of Global Ecology, Carnegie Institution for Science, Stanford, California, USA, [2]Bodega Marine Laboratory, University of California Davis, Davis, California, USA, [3]Department of Earth and Planetary Sciences, University of California Davis, Davis, California, USA, [4]Department of Evolution and Ecology, University of California Davis, Davis, California, USA, [5]The Interuniversity Institute for Marine Sciences, Eilat, The H. Steinitz Marine Biology Laboratory, Hebrew University of Jerusalem, Jerusalem, Israel, [6]The Fredy and Nadine Herrman Institute of Earth Sciences, Hebrew University of Jerusalem, Jerusalem, Israel, [7]School of Medical Sciences, University of Sydney, Sydney, New South Wales, Australia

Abstract Ocean acidification has the potential to adversely affect marine calcifying organisms, with substantial ocean ecosystem impacts projected over the 21st century. Characterizing the in situ sensitivity of calcifying ecosystems to natural variability in carbonate chemistry may improve our understanding of the long-term impacts of ocean acidification. We explore the potential for intensive temporal sampling to isolate the influence of carbonate chemistry on community calcification rates of a coral reef and compare the ratio of organic to inorganic carbon production to previous studies at the same location. Even with intensive temporal sampling, community calcification displays only a weak dependence on carbonate chemistry variability. However, across three years of sampling, the ratio of organic to inorganic carbon production is highly consistent. Although further work is required to quantify the spatial variability associated with such ratios, this suggests that these measurements have the potential to indicate the response of coral reefs to ongoing disturbance, ocean acidification, and climate change.

1. Introduction

1.1. The Sensitivity of Community Calcification to Carbonate Chemistry Variability

Ocean acidification occurs as a consequence of the anthropogenic emissions of CO_2 and the uptake of a proportion of this CO_2 into the oceans [*Caldeira and Wickett*, 2003]. This process results in a decrease in seawater pH and a lowering of the calcium carbonate saturation state (Ω) [*Doney et al.*, 2009]. Ocean acidification is considered a major threat to many marine organisms and in particular calcifying species, which can be strongly influenced by Ω [*Orr et al.*, 2005; *Kleypas et al.*, 2006; *Kwiatkowski et al.*, 2015].

The long-term sensitivity of calcifying communities to ocean acidification is of great ecological and economic interest [*Kroeker et al.*, 2013]. Laboratory experiments have shown that the calcification of many species declines with lower Ω [*Marubini and Atkinson*, 1999; *Leclercq et al.*, 2000; *Langdon and Atkinson*, 2005; *Kroeker et al.*, 2013]. Determining the level of community sensitivity in situ is more difficult and, although there are emerging manipulation studies [*Albright et al.*, 2016], has been largely dependent on the analysis of study sites with volcanic CO_2 seeps that produce strong spatial gradients in calcium carbonate saturation state [*Hall-Spencer et al.*, 2008; *Fabricius et al.*, 2011] or sites that are isolated from the open ocean during low tide and can therefore experience large temporal variability in Ω due to localized photosynthesis and respiration [*Silverman et al.*, 2012; *Shaw et al.*, 2015; *Kwiatkowski et al.*, 2016]. The latter of these approaches is the focus of this study.

Here we conduct slack-water carbonate chemistry measurements to determine the influence of natural variability in aragonite saturation state (Ω_{arag}) on aggregated community calcification rates. Compared to previous attempts to characterize such relationships in 2009 [*Silverman et al.*, 2012] and 2013 [*Shaw et al.*, 2015] at the same location, our sampling frequency was 3–5 times higher, resulting in 2.5–8.5 times the total number of seawater samples. Given that constraining relationships between seawater chemistry and community calcification are inherently difficult due to multicollinearity between drivers of calcification such as light, temperature, and carbonate chemistry [*Jokiel et al.*, 2014], higher-frequency sampling [e.g., *McMahon et al.*, 2013], made possible through the use of an automated water sampler, should be more effective at isolating the in situ influence of Ω_{arag} on community calcification rates.

1.2. Alkalinity (A_T) and Dissolved Inorganic Carbon (C_T) Ratios as Indicators of Reef Health

The analysis of A_T/C_T diagrams was first introduced as a means to solve a variety of carbonate system equilibrium problems [*Deffeyes*, 1965]. In coral reef environments A_T/C_T regression slopes are predominately influenced by net calcification (calcification minus dissolution) and net production (photosynthesis minus respiration) and therefore reflect the ratio of organic to inorganic carbon cycling [*Suzuki et al.*, 2001].

A_T/C_T diagrams have been used to understand organic and inorganic carbon budgets, and how reef systems can act as alkalinity sinks and sources of atmospheric CO_2 [*Suzuki et al.*, 2001; *Suzuki and Kawahata*, 2003], often when reliable estimates of seawater mass fluxes have been difficult. They have also been used to indicate the impact of coral bleaching and predation on community calcification [*Watanabe et al.*, 2006]. More recently, A_T/C_T regression slopes have been shown to differ between coral-dominated and algal-dominated reef flats [*Lantz et al.*, 2014] as a result of greater relative net community calcification in coral-dominated environments. This has prompted the advocation of consistent A_T/C_T measurements as a means of assessing the long-term impact of anthropogenic stressors and particularly climate change on coral reefs [*Albright et al.*, 2013; *Lantz et al.*, 2014; *Shaw et al.*, 2015].

Reef communities can shift from a state of high coral cover to a coral depauperate state and higher macroalgal cover as a consequence of stressors such as disease [*Mumby et al.*, 2007], disturbance [*Roff et al.*, 2015], and climate change [*Hoegh-Guldberg et al.*, 2007]. It has been proposed that such phase shifts would increase the ratio of organic to inorganic carbon cycling. Consequently, A_T/C_T ratios could act as salient indicators of the health of reef ecosystems [*Albright et al.*, 2013; *Lantz et al.*, 2014; *Shaw et al.*, 2015]. This, however, assumes that given limited changes in community composition, A_T/C_T ratios are relatively stable ecosystem features that do not show strong spatial or temporal variability. We test the assumption of limited temporal variability by exploring how A_T/C_T ratios differ between our data set and those previously collected on the same reef flat in 2009 [*Silverman et al.*, 2012] and 2013 [*Shaw et al.*, 2015].

2. Materials and Methods

### 2.1. Experimental Protocol

Our study site was the nominally named DK13 location [*Kinsey*, 1979] of One Tree Island, Australia (23°30′S, 152°06′E). At low tide, the water level drops below the height of the reef crest, and the study site is isolated from the open ocean for 4–6 hr, permitting measurements of carbonate chemistry that reflect local biogeochemistry. From 12 September 2014 to 10 October 2014, an automated water sampler was deployed on the reef flat and programmed to collect seawater samples (as described in *Albright et al.* [2013]) at approximately 50 min intervals, beginning 2 hr before each low tide and ending 2 hr after each low tide. Depth was approximately 0.45 m at the start of low tide periods and approached 0.36 m by the end of low tide periods. The mean depths of sampling locations were 0.8 m [*Silverman et al.*, 2012] and 0.55 m [*Shaw et al.*, 2015] in the previous DK13 studies. The autosampler location in this study was approximately 25 m and 400 m from the sampling stations of *Silverman et al.* [2012] and *Shaw et al.* [2015], respectively. The percent cover of key functional groups was estimated using a point intercept transect method, consistent with previous studies [*Kinsey*, 1979; *Silverman et al.*, 2012].

2.2. Carbonate System and Nutrient Measurements

Seawater samples were analyzed for total alkalinity (A_T), pH, and dissolved inorganic carbon (C_T). The C_T, pCO_2, CO_3^{2-}, and Ω_{arag} values were calculated from A_T, pH, salinity, and temperature using the CO2SYS program [*Lewis and Wallace*, 1998] with calculated C_T values validated against measurements. The K_1 and K_2 constants of *Mehrbach* [1973] refit by *Dickson and Millero* [1987] were utilized, and total boron was calculated using the B/chlorinity ratio of *Uppström* [1974]. Expanded descriptions of carbonate chemistry measurement protocols are given in the supporting information.

2.3. Net Community Calcification and Production

Net community calcification (G_{net}) was estimated using the alkalinity anomaly method developed by *Kinsey* [1978] and adopted in previous studies at the same location [*Silverman et al.*, 2012; *Shaw et al.*, 2015]. Samples taken after depth started to increase and during rain were excluded from analysis. The uncertainty in G_{net} and P_{net} estimates was calculated using the measurement errors in A_T and pH to derive the propagated error in
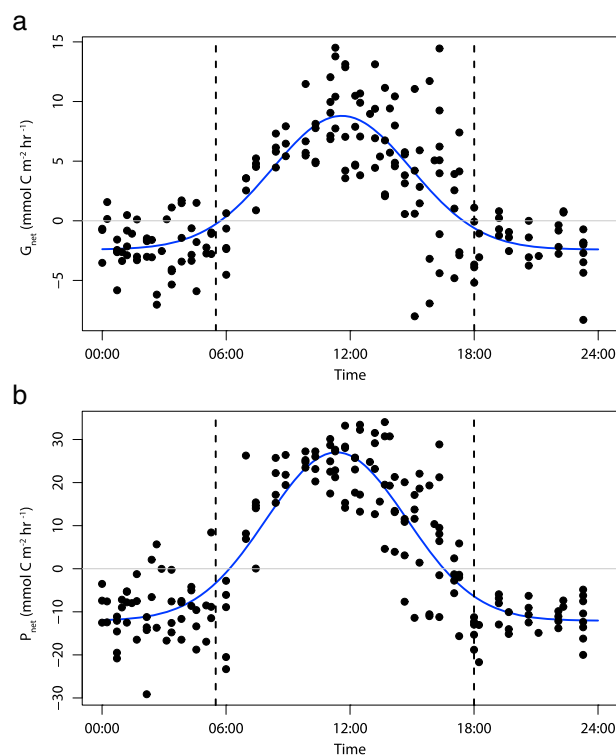
Figure 1. Temporal cycles in community calcification (G_{net}) and production (P_{net}). (a) G_{net} (mmol C m^{-2} hr^{-1}) and (b) P_{net} (mmol C m^{-2} hr^{-1}) against time of day. Dashed lines indicate approximate daylight hours during the study period. Values outside the hourly mean ± 2 standard deviations of the mean are not shown.
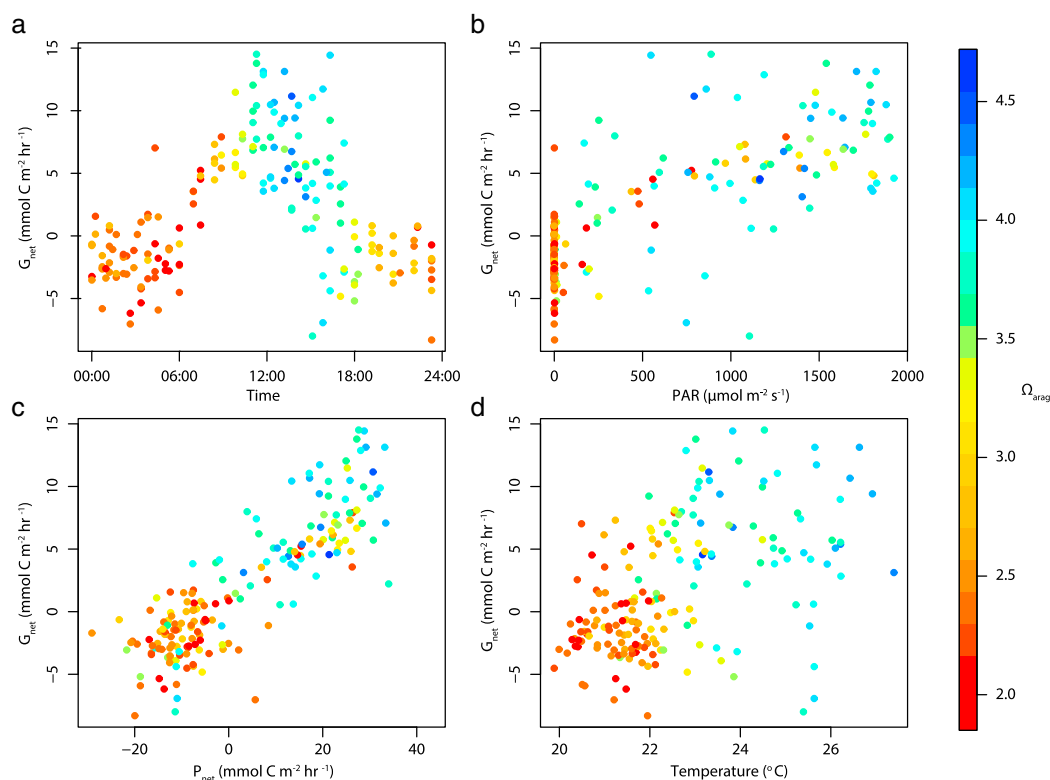
calculated C_T values and assuming a relative depth uncertainty of 20%. Alternative methods for estimating G_{net} and P_{net} fluxes using the least squares regression slope of all samples taken during a low tide [*McMahon et al.*, 2013] are compared in the supporting information.

2.4. Statistical Modeling

Linear least squares regression models were used to determine the influence of P_{net}, PAR, temperature, and Ω_{arag} on G_{net}. Model selection was based on minimizing model AIC. Thus,

$$G_{net} = \beta_0 + \beta_1(P_{net}) + \beta_2(\text{PAR}) + \beta_3(T) + \beta_4(\Omega_{arag}) + \varepsilon \qquad (1)$$

where Ω_{arag} is the mean of the Ω_{arag} values measured in two consecutive sampling times, photosynthetically active radiation (PAR) is the mean PAR between two sampling times, and T is the mean temperature between two sampling times. We note that this approach assumes a linear dependence of G_{net} on Ω_{arag} that while typically observed in the laboratory [e.g., *Langdon et al.*, 2000; *Leclercq et al.*, 2000] may not be present in situ [*McMahon et al.*, 2013].

3. Results

A total of 273 separate seawater samples was analyzed for carbonate chemistry parameters with samples taken during rainfall not analyzed. Of these, five samples were deemed highly anomalous (i.e., carbonate chemistry parameters were >2 standard deviations from the mean) and discarded. The diel variability in carbonate chemistry parameters is shown in Figure S5 in the supporting information.

3.1. Community Calcification and Sensitivity to Ω_{arag}

The diel cycles in G_{net} and P_{net} are shown in Figure 1. Over the sampling period, net 24 h calcification and production, calculated as the integral of mean G_{net} and P_{net} functions, were 36.3 ± 9.5 mmol C m^{-2} d^{-1} (±1 standard deviation) and 41.7 ± 21.6 mmol C^{-1} m^{-2} d^{-1}, respectively. During daylight hours mean G_{net} and P_{net} were 4.7 ± 1.1 mmol C m^{-2} hr^{-1} and 12.7 ± 5.7 mmol C m^{-2} hr^{-1}, while at night mean G_{net} and P_{net} were -1.9 ± 0.6 mmol C m^{-2} hr^{-1} and -10.2 ± 6.1 mmol C m^{-2} hr^{-1}, respectively. The mean rate of daytime calcification was therefore approximately 2.45 times the rate of nighttime dissolution. Thus, during the study period the reef was in a state of net calcification despite consistent nighttime dissolution of CaCO$_3$ (i.e., negative G_{net}) and in a state of net autotrophy despite consistent nighttime respiration (i.e., negative P_{net}). The G_{net} values estimated here are on the low end of the reported range of values for reef flats (20–250 mmol C m^{-2} d^{-1}) [*Atkinson*, 2011]. Estimated net community production (P_{net}) values are within the previously reported range of reef flats (−200 to 280 mmol C m^{-2} d^{-1}) [*Atkinson*, 2011], but as discussed below, implied respiration and gross production rates are substantially lower than measured at this study site by *Silverman et al.* [2012] and *Kinsey* [1979].

Summary results of the statistical modeling of G_{net} are given in Table S2. The optimal model based on minimizing AIC values uses PAR, P_{net}, and Ω_{arag} with temperature (T) found to confer no additional explanatory power. However, when both variabilities in PAR and P_{net} are accounted for, variability in Ω_{arag} explains only

Figure 2. Rate of community calcification (G_{net}; mmol C m^{-2} hr^{-1}) against (a) time of day, (b) photosynthetically active radiation (μmol m^{-2} s^{-1}), (c) community production (P_{net}; mmol C m^{-2} hr^{-1}), and (d) temperature (°C). Point color indicates the in situ aragonite saturation state (Ω_{arag}).

1% of the residual variability in community calcification rates. Natural variability in Ω_{arag} is therefore only a weak driver of short-term variability in G_{net} with most variability explained by PAR and/or P_{net}. Multicollinearity between explanatory variables was tested with variance inflation factors (VIFs). PAR, P_{net}, and Ω_{arag} were found to have VIFs of 3.13, 2.23, and 1.88, respectively. As such, it is justifiable to include all three explanatory variables based on all accepted VIF thresholds [*Hair*, 2006; *Pan and Jackson*, 2008]. Our approach does, however, assume an idealized independence between variables which is likely not present in situ. For example, changes in temperature during the daytime are largely driven by solar radiation, and there are likely feedbacks between G_{net} and the explanatory variables P_{net} and Ω_{arag}. The statistical modeling results should therefore be interpreted with caution.

Figure 2 shows how the relationship between Ω_{arag} and G_{net} is influenced by time of day, PAR, P_{net}, and temperature. The highest G_{net} values were observed around 12:00 P.M. when P_{net}, PAR, temperature, and Ω_{arag} values were also high. Peak Ω_{arag} values were observed around 2:00 P.M. later in the day than peak G_{net} values. At a given P_{net}, PAR, or temperature value there is a large range in G_{net}; however, it is difficult to discern a clear relationship between the magnitude of G_{net} and in situ Ω_{arag}. This highlights the difficulty in determining a robust signal of Ω_{arag} on G_{net} and reinforces the result that Ω_{arag} has only a weak influence on short-term, diel variability in G_{net}.

3.2. Organic to Inorganic Carbon Production Ratios

The ratio of organic to inorganic carbon production is estimated from a total least squares linear regression of absolute values of alkalinity (A_T) against dissolved inorganic carbon (C_T). The slope of the regression is 0.45 ± 0.01 which is an organic to inorganic carbon production ratio of 3.44 (Figure 3). This is within the uncertainty bounds of the [*Silverman et al.*, 2012] data set collected in 2009, which has a slope of 0.46 ± 0.02 and an organic to inorganic carbon production ratio 3.35. However, our results, although similar, fall slightly outside the uncertainty bounds of the [*Shaw et al.*, 2015] data set collected in 2013 which has a slope of 0.39 ± 0.04
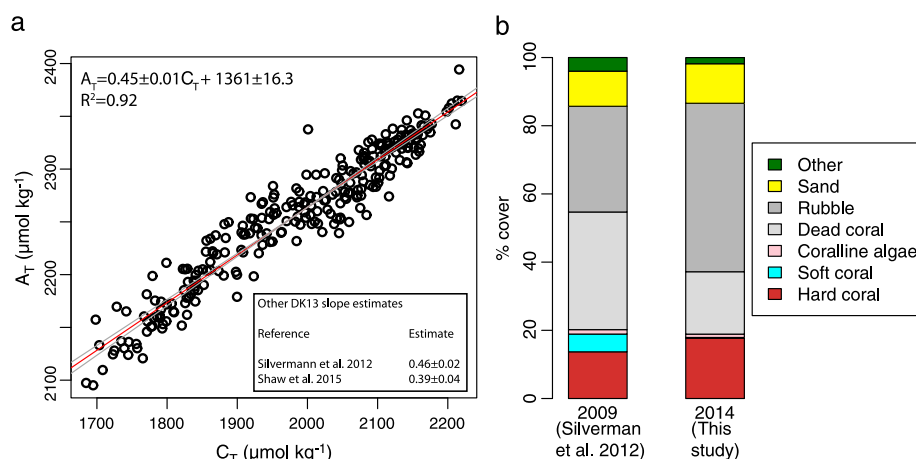
Figure 3. (a) Total least squares regression of alkalinity (A_T) against dissolved inorganic carbon (C_T) with comparative estimates of regression slopes from previous studies at the same location shown and (b) benthic community composition estimates in 2009 [*Silverman et al.*, 2012] and 2014 based on a linear point intercept method. Comparable community composition estimates are not available in 2013 [*Shaw et al.*, 2015].

and an organic to inorganic carbon production ratio of 4.13. There was limited difference between daytime A_T/C_T regression slopes (0.46 ± 0.01) and nighttime A_T/C_T regression slopes (0.50 ± 0.03) during our study (Figure S7).

The benthic composition of the DK13 study site location was reassessed using a similar methodology to previous studies [*Silverman et al.*, 2012]. Figure 3b shows that between 2009 and 2014 there were limited changes in the percentage cover of benthic categories. We estimated slightly higher hard coral cover ($17.7 \pm 2.4\%$) that was recorded in 2009 ($13.7 \pm 3.2\%$) [*Silverman et al.*, 2012], and the extent of soft coral cover ($0.2 \pm 0.2\%$) was lower than that estimated in 2009 ($5.2 \pm 2.2\%$). These differences in benthic composition are relatively minor and within uncertainty bounds inherent in the point intercept transect method used. The benthic composition within the estimated effective footprint area of metabolism measurements ($10-15$ m from the autosampler) was representative of the larger transect area (Figure S8). Comparable community composition estimates in 2013 are not provided in Shaw *et al.* [2015]. However, benthic community composition at the scale of broad ecosystem functional types is assumed to have remained relatively stable across all three studies (2009–2014).

4. Discussion and Conclusions

4.1. Community Calcification and Sensitivity to Ω_{arag}

As a consequence of an intensive sampling protocol at the DK13 reef site in 2014, the data set presented in this study contains 2.6 times as many seawater samples as data sets collected at the same location in 2009 and 8.5 times as many samples as collected in 2013. This allowed for a more robust assessment of the variability in low tide carbonate chemistry parameters and the associated variability in community calcification and production rates. In September–October 2014 we measured mean G_{net} and P_{net} values of 36.3 ± 9.5 mmol C m^{-2} d^{-1} and 41.7 ± 21.6 mmol C m^{-2} d^{-1}, respectively. These values differ from those measured by *Silverman et al.* [2012] in November–December 2009 (G_{net}: 74 mmol C m^{-2} d^{-1} and P_{net}: 18 mmol C m^{-2} d^{-1}) but are similar to those measured by *Shaw et al.* [2015] in November 2013 (G_{net}: 33 mmol C m^{-2} d^{-1} and P_{net}: 35 mmol C m^{-2} d^{-1}). All G_{net} measurements made in 2009–2014 are 26–59% of the mean annual values measured between 1967 and 1975 [*Kinsey*, 1979] (G_{net}: 126 mmol C m^{-2} d^{-1}). These lower community calcification measurements may be a consequence of chronic stressors such as rising sea surface temperatures and ocean acidification over the last 40 years as posited by *Silverman et al.* [2012]; however, without detailed knowledge of the spatial variability in G_{net} along the reef flat, such a conclusion is highly tentative.

The daily respiration rate (R) is calculated as the mean hourly nighttime P_{net} (the respiration baseline) integrated over 24 hr, while gross production (P) is calculated as the integrated P_{net} during daylight hours in

addition to the integrated respiration baseline over this period [*Marsh and Smith*, 1978]. Our measurements imply an R of 244.8 ± 146.4 mmol C m^{-2} d^{-1} and P of 285.6 ± 104.4 mmol C m^{-2} d^{-1}. These values are also substantially lower than those of *Silverman et al.* [2012] (P: 788 mmol C m^{-2} d^{-1} and R: 780 mmol C m^{-2} d^{-1}) and those of *Kinsey* [1979] (P: 616 mmol C m^{-2} d^{-1} and R: 600 mmol C m^{-2} d^{-1}). Comparable values of R and P are not provided by *Shaw et al.* [2015]. As discussed in greater detail below, numerous uncertainties associated with G_{net}, P_{net}, P, and R estimates likely preclude meaningful comparisons between previous studies.

The statistical modeling of community calcification rates shows that the optimal model based on minimizing AIC values uses PAR, P_{net}, and Ω_{arag} (Table S2). All variable coefficients have positive signs indicating higher community calcification rates at higher community production rates, higher PAR levels, and higher Ω_{arag} conditions, respectively. Coefficient signs are therefore broadly consistent with aquaria experiments and in particular those that have shown higher calcification rates at higher Ω_{arag} [e.g., *Leclercq et al.*, 2000; *Langdon et al.*, 2000].

We find that the majority (62%) of variability in net community calcification rates (G_{net}) can be explained by PAR and community production rates (P_{net}), with carbonate saturation state (Ω_{arag}) only explaining a small amount (1%) of the residual variability. Ω_{arag} is therefore a very weak driver of short-term variability in net community calcification rates as has been documented at other reefs [e.g., *Falter et al.*, 2012]. Despite our sample size ($N = 273$) being almost an order of magnitude greater than the data set taken in 2013 [*Shaw et al.*, 2015] ($N = 32$), our findings are broadly similar, albeit with model explanatory power ($R^2 = 0.63$) that is lower ($R^2 = 0.95$). Our data set does not allow one to distinguish between the competing influences of calcification and dissolution on net community calcification (G_{net}). Biologically mediated calcification processes may exhibit greater resilience to Ω_{arag} variability than dissolution processes which are mainly a geochemical response to seawater chemistry changes [*Eyre et al.*, 2014]. The influence of Ω_{arag} on G_{net} that we describe may therefore be driven by greater calcium carbonate dissolution, most likely in reef sediments [*Cyronak et al.*, 2013] and not solely calcification processes.

It is important to note that our estimates of the short-term sensitivity of net community calcification to Ω_{arag} variability may only partially reflect the long-term sensitivity of such communities to ongoing ocean acidification. The sensitivity of certain organisms to Ω_{arag} in manipulative aquaria experiments has been shown to depend on experimental duration [*Ragazzola et al.*, 2013]. In addition, the aggregated long-term impact of ocean acidification on coral reef ecosystems will not be limited to net community calcification, with potential additional impacts on survival and reproduction [*Kroeker et al.*, 2013].

4.2. Uncertainties in G_{net} and P_{net} Estimates

Estimating diel G_{net} and P_{net} values in situ is prone to biases and large errors that are often inherent to the hyrdodynamic assumptions underlying the methodological approach [*Zhang et al.*, 2012; *Lowe and Falter*, 2015] and are difficult to characterize. At the same DK13 field location, the choice of slack-water measurements as opposed to Lagrangian flow measurements can cause a threefold difference in mean daytime G_{net} values [*Shaw et al.*, 2014]. Some of these differences may be due to the direct influence of differing flow rates on calcification [*Comeau et al.*, 2014; *Cornwall et al.*, 2014] in addition to inaccuracies in characterizing complex, often nonunidirectional, flow regimes [*Shaw et al.*, 2014]. Uncertainty in bottom depth over small spatial scales can also affect G_{net} and P_{net} estimates [*Shaw et al.*, 2014] and limit comparisons between studies at different locations. Table S4 shows how idealized levels of uncertainty in depth would influence the measurement uncertainty of our G_{net} and P_{net} estimates which previously assumed 20% relative uncertainty in depth. The greatest uncertainty in such metabolism measurements, however, likely relates to reef surface area. The total surface area of reefs can be more than an order of magnitude greater than the two-dimensional area and vary substantially over small spatial scales [*Dahl*, 1973]. G_{net} and P_{net} estimates are typically calculated in planar area units, and therefore, small differences in sampling location and contemporaneously reef rugosity have the potential to greatly influence values.

G_{net} and P_{net} estimates from different studies at the same location are likely to have different effective footprints depending on site location, wind speeds, flow regimes, and the time between consecutive samples. Measuring the movement of fluorescein dye injections, we estimated low tide flow rates of ~0.33 cm s^{-1} at the sampling site consistent with *Silverman et al.* [2012] who estimate low tide flow rates of 0.6 ± 0.7 cm s^{-1}.

Dye dispersion and advection resulted in a tenfold decrease in concentration within 10 min at the site of dye release (Figure S3). The low flow speeds demonstrated by the movement of dye patches (~0.33 cm s^{-1}) suggest that the changes in carbonate chemistry we observed were dominated by local reef metabolism rather than by the advection of new water with differing chemistry. Furthermore, the fact that dye concentrations decreased by ~95% after advecting just 2 m in 10 min (Figure S3) suggests that there was more than enough ambient turbulence to vertically mix the water column; at least over the timescale of our benthic metabolism measurements [*Lowe and Falter*, 2015]. Given that the time between consecutive samples is approximately 50 min, our flow rate equates to an effective footprint of our G_{net} and P_{net} point measurements of ~10 m in radius but this will differ from that of other DK13 studies [*Kinsey*, 1979; *Silverman et al.*, 2012; *Shaw et al.*, 2015] which had nonidentical sampling locations along the same back reef and longer time intervals between consecutive water samples. Future reef metabolism studies would benefit from explicitly estimating footprints using Acoustic Doppler Velocimeters [e.g., *Long et al.*, 2013] to establish measurement reproducibility.

Further uncertainties in diel G_{net} and P_{net} estimates relate to sample sizes and curve fitting procedures. For practical reasons, without the use of autosamplers, fewer measurements are typically taken, and especially so during the night. Limitations on study duration and the total number of carbonate chemistry samples that can be analyzed mean that many studies fail to document the uncertainty in G_{net} at a given time of day which can encompass up to an order of magnitude (Figure 1) [*Silverman et al.*, 2012; *Albright et al.*, 2015]. Studies which fail to characterize such natural variability due to limited sampling will be highly prone to errors in G_{net} and P_{net} estimates. Given the extensive uncertainties associated with integrated G_{net} and P_{net} estimates, it is difficult to robustly compare values across studies. As such no inferences are made with regard to the difference between our G_{net} and P_{net} estimates and those of Silverman *et al.* [2012] and Shaw *et al.* [2015].

4.3. Organic to Inorganic Carbon Production Ratios

The ratio of organic to inorganic carbon production across coral reefs has been shown to vary seasonally [*Kinsey*, 1979; *Smith*, 1981; *Atkinson and Grigg*, 1984; *Albright et al.*, 2013]; however, the interannual variability in such ratios has not been characterized. We show that on the same reef flat organic to inorganic carbon production ratios are largely consistent across the three sampling periods: November–December 2009 (3.35), November 2013 (4.13), and September–October 2014 (3.44). These organic to inorganic carbon production ratios fall centrally within the range of values published for other coral reefs (2.0–6.7) [*Gattuso et al.*, 1996; *Albright et al.*, 2013; *Lantz et al.*, 2014; *Shaw et al.*, 2015]. Despite both net community production and net community calcification being generally positive during the day and negative during the night (Figure 1) and both A_T and C_T values being typically elevated during the night (Figure S5) [*Suzuki and Kawahata*, 2003], we find that A_T/C_T regression slopes taken during the day and the night are indistinguishable. This indicates that the ratio of organic to organic carbon cycling was largely consistent over diel cycles.

During the period November 2009 to October 2014 the benthic community structure of the reef, as estimated by a point intercept transect method, was largely unchanged (Figure 3b). Therefore, it appears that at least at this location and time of year, there is limited interannual variability in organic to inorganic carbon production ratios. The differing exact sampling location of each study has the potential to cause spatially dependent differences in organic to inorganic carbon production ratios, and yet no large differences were observed (Figure 3a). As such ratios are not based on ΔA_T and ΔC_T values but absolute A_T and C_T measurements they have a larger effective footprint. In our study mean flow rates were estimated as ~0.33 cm s^{-1}, and therefore, over a low tide period of 4–6 hr this effective footprint is estimated as being 48–72 m in radius (~5–7 times the radius of the effective footprint of our G_{net} and P_{net} measurements). This may explain the consistency between our organic to inorganic carbon production ratios and those of *Silverman et al.* [2012] and *Shaw et al.* [2015]. However, we cannot rule out that measurement similarities were coincidental. Further work is required to establish the precise effective footprints of organic to inorganic carbon production ratios and quantify the extent of their spatial variability.

The consistency of organic to inorganic carbon production ratios indicates that the ability of this reef system to modify seawater pH and Ω_{arag}, which has the potential to partially offset some of the changes in seawater chemistry due to ocean acidification [*Andersson et al.*, 2014], has remained unchanged over the last five years.

The stability of these ratios also indicates that they are relatively stable ecosystem features that could act as robust indicators of the health of reef ecosystems. An increase in organic to inorganic carbon production rates on a reef could exacerbate the impact of ocean acidification by contributing to larger diel variability in pH and Ω_{arag}. However, organic to inorganic carbon production ratios only reflect the ratio of net community production to net community calcification and therefore consistent ratios may mask compensating changes in reef metabolism that are not revealed by such analyses (e.g., increases in calcification in combination with increases in dissolution).

If a change in the organic to inorganic carbon production ratio is recorded at a given location, this is only an initial step in evaluating potential reef degradation or indeed recovery from some disturbance. Further analysis is required to determine whether this is a consequence of a number of processes including changes in bioerosion, bleaching, or chronic anthropogenic stressors such as ocean acidification and rising sea surface temperatures. Long-term monitoring of carbonate chemistry parameters could nonetheless highlight changes in ecosystem function in response to stressors such as pollution, overfishing, ocean acidification, and climate change.

References

Albright, R., C. Langdon, and K. R. N. Anthony (2013), Dynamics of seawater carbonate chemistry, production, and calcification of a coral reef flat, central Great Barrier Reef, *Biogeosciences*, *10*(10), 6747–6758, doi:10.5194/bg-10-6747-2013.

Albright, R., J. Benthuysen, N. Cantin, K. Caldeira, and K. Anthony (2015), Coral reef metabolism and carbon chemistry dynamics of a coral reef flat, *Geophys. Res. Lett.*, *42*, 3980–3988, doi:10.1002/2015GL063488.

Albright, R., et al. (2016), Reversal of ocean acidification enhances net coral reef calcification, *Nature*, doi:10.1038/nature17155.

Andersson, A. J., K. L. Yeakel, N. R. Bates, and S. J. de Putron (2014), Partial offsets in ocean acidification from changing coral reef biogeochemistry, *Nat. Clim. Change*, *4*(1), 56–61, doi:10.1038/nclimate2050.

Atkinson, M. (2011), *Biogeochemistry of Nutrients, in Coral Reefs: An Ecosystem in Transition*, Springer, Netherlands.

Atkinson, M. J., and R. W. Grigg (1984), Model of a coral reef ecosystem, *Coral Reefs*, *3*(1), 13–22, doi:10.1007/BF00306136.

Caldeira, K., and M. E. Wickett (2003), Oceanography: Anthropogenic carbon and ocean pH, *Nature*, *425*(6956), 365–365, doi:10.1038/425365a.

Comeau, S., P. J. Edmunds, C. A. Lantz, and R. C. Carpenter (2014), Water flow modulates the response of coral reef communities to ocean acidification, *Sci. Rep.*, *4*, doi:10.1038/srep06681.

Cornwall, C. E., P. W. Boyd, C. M. McGraw, C. D. Hepburn, C. A. Pilditch, J. N. Morris, A. M. Smith, and C. L. Hurd (2014), Diffusion boundary layers ameliorate the negative effects of ocean acidification on the temperate coralline macroalga arthrocardia corymbosa, *PLoS One*, *9*(5), e97235, doi:10.1371/journal.pone.0097235.

Cyronak, T., I. R. Santos, and B. D. Eyre (2013), Permeable coral reef sediment dissolution driven by elevated pCO2 and pore water advection, *Geophys. Res. Lett.*, *40*, 4876–4881, doi:10.1002/grl.50948.

Dahl, A. L. (1973), Surface area in ecological analysis: Quantification of benthic coral-reef algae, *Mar. Biol.*, *23*(4), 239–249, doi:10.1007/BF00389331.

Deffeyes, K. S. (1965), Carbonate equilibria: A graphic and algebraic approach 1, *Limnol. Oceanogr.*, *10*(3), 412–426, doi:10.4319/lo.1965.10.3.0412.

Dickson, A. G., and F. J. Millero (1987), A comparison of the equilibrium constants for the dissociation of carbonic acid in seawater media, *Deep Sea Res. Part Oceanogr. Res. Paper*, *34*(10), 1733–1743, doi:10.1016/0198-0149(87)90021-5.

Doney, S. C., V. J. Fabry, R. A. Feely, and J. A. Kleypas (2009), Ocean acidification: The other CO_2 problem, *Ann. Rev. Mar. Sci.*, *1*(1), 169–192, doi:10.1146/annurev.marine.010908.163834.

Lewis, E., and D. W. R. Wallace (1998), Program developed for CO2 system calculations, Carbon Dioxide Information Analysis Center, Oak Ridge National Laboratory, U.S. Dep. of Energy, Oak Ridge, Tenn.

Eyre, B. D., A. J. Andersson, and T. Cyronak (2014), Benthic coral reef calcium carbonate dissolution in an acidifying ocean, *Nat. Clim. Change*, *4*(11), 969–976, doi:10.1038/nclimate2380.

Fabricius, K. E., C. Langdon, S. Uthicke, C. Humphrey, S. Noonan, G. De'ath, R. Okazaki, N. Muehllehner, M. S. Glas, and J. M. Lough (2011), Losers and winners in coral reefs acclimatized to elevated carbon dioxide concentrations, *Nat. Clim. Change*, *1*(3), 165–169, doi:10.1038/nclimate1122.

Falter, J. L., R. J. Lowe, M. J. Atkinson, and P. Cuet (2012), Seasonal coupling and de-coupling of net calcification rates from coral reef metabolism and carbonate chemistry at Ningaloo Reef, Western Australia, *J. Geophys. Res.*, *117*, C05003, doi:10.1029/2011JC007268.

Gattuso, J.-P., M. Pichon, B. Delesalle, C. Canon, and M. Frankignoulle (1996), Carbon fluxes in coral reefs. I. Lagrangian measurement of community metabolism and resulting air-sea CO2 disequilibrium, *Mar. Ecol. Prog. Ser.*, *145*, 109–121, doi:10.3354/meps145109.

Hair, J. F. (2006), *Multivariate Data Analysis*, Pearson Prentice Hall, Upper Saddle River, N. J.

Hall-Spencer, J. M., R. Rodolfo-Metalpa, S. Martin, E. Ransome, M. Fine, S. M. Turner, S. J. Rowley, D. Tedesco, and M.-C. Buia (2008), Volcanic carbon dioxide vents show ecosystem effects of ocean acidification, *Nature*, *454*(7200), 96–99, doi:10.1038/nature07051.

Hoegh-Guldberg, O., et al. (2007), Coral reefs under rapid climate change and ocean acidification, *Science*, *318*(5857), 1737–1742, doi:10.1126/science.1152509.

Jokiel, P. L., C. P. Jury, and K. S. Rodgers (2014), Coral-algae metabolism and diurnal changes in the CO2-carbonate system of bulk sea water, *PeerJ*, *2*, e378, doi:10.7717/peerj.378.

Kinsey, D. W. (1978), Productivity and calcification estimates using slackwater period and field enclosures, *in Coral Reef Research Methods, Monogr. on Oceanogr. Methodol. 5*, UNESCO, Paris.

Kinsey, D. W. (1979), Carbon turnover and accumulation by coral reefs, PhD thesis, Univ. of Hawai'i, Honolulu.

Kleypas, J., R. Feely, V. Fabry, C. Langdon, C. Sabine, and L. Robbins (2006), Impacts of ocean acidification on coral reefs and other marine calcifiers. *A Guide for Future Research. Report of a Workshop Sponsored by NSF, NOAA & USGS.*

Kroeker, K. J., R. L. Kordas, R. Crim, I. E. Hendriks, L. Ramajo, G. S. Singh, C. M. Duarte, and J.-P. Gattuso (2013), Impacts of ocean acidification on marine organisms: Quantifying sensitivities and interaction with warming, *Glob. Change Biol.*, *19*(6), 1884–1896, doi:10.1111/gcb.12179.

Kwiatkowski, L., P. Cox, P. R. Halloran, P. J. Mumby, and A. J. Wiltshire (2015), Coral bleaching under unconventional scenarios of climate warming and ocean acidification, *Nat. Clim. Change*, *5*(8), 777–781, doi:10.1038/nclimate2655.

Kwiatkowski, L., et al. (2016), Nighttime dissolution in a temperate coastal ocean ecosystem increases under acidification, *Sci. Rep.*, *6*, 22984, doi:10.1038/srep22984.

Langdon, C., and M. J. Atkinson (2005), Effect of elevated pCO2 on photosynthesis and calcification of corals and interactions with seasonal change in temperature/irradiance and nutrient enrichment, *J. Geophys. Res.*, *110*, C09S07, doi:10.1029/2004JC002576.

Langdon, C., T. Takahashi, C. Sweeney, D. Chipman, J. Goddard, F. Marubini, H. Aceves, H. Barnett, and M. J. Atkinson (2000), Effect of calcium carbonate saturation state on the calcification rate of an experimental coral reef, *Global. Biogeochem. Cycles*, *14*(2), 639–654, doi:10.1029/1999GB001195.

Lantz, C. A., M. J. Atkinson, C. W. Winn, and S. E. Kahng (2014), Dissolved inorganic carbon and total alkalinity of a Hawaiian fringing reef: Chemical techniques for monitoring the effects of ocean acidification on, *Coral Reefs*, *33*(1), 105–115, doi:10.1007/s00338-013-1082-5.

Leclercq, N., J.-P. Gattuso, and J. Jaubert (2000), CO2 partial pressure controls the calcification rate of a coral community, *Global Change Biol.*, *6*(3), 329–334, doi:10.1046/j.1365-2486.2000.00315.x.

Long, M. H., P. Berg, D. de Beer, and J. C. Zieman (2013), In situ coral reef oxygen metabolism: An eddy correlation study, *PLoS One*, *8*(3), e58581, doi:10.1371/journal.pone.0058581.

Lowe, R. J., and J. L. Falter (2015), Oceanic forcing of coral reefs, *Ann. Rev. Mar. Sci.*, *7*(1), 43–66, doi:10.1146/annurev-marine-010814-015834.

Marsh, J. A. J., and S. V. Smith (1978), Productivity measurements of coral reefs in flowing waters, in *Coral Reefs: Research Methods*, pp. 361–377, UNESCO, Paris.

Marubini, F., and M. J. Atkinson (1999), Effects of lowered pH and elevated nitrate on coral calcification, *Mar. Ecol. Prog. Ser.*, *188*, 117–121, doi:10.3354/meps188117.

McMahon, A., I. R. Santos, T. Cyronak, and B. D. Eyre (2013), Hysteresis between coral reef calcification and the seawater aragonite saturation state, *Geophys. Res. Lett.*, *40*, 4675–4679, doi:10.1002/grl.50802.

Mehrbach, C. (1973), Measurement of the apparent dissociation constants of carbonic acid in seawater at atmospheric pressure, *Limnol. Oceanogr.*, *18*(6), 897–907, doi:10.4319/lo.1973.18.6.0897.

Mumby, P. J., A. Hastings, and H. J. Edwards (2007), Thresholds and the resilience of Caribbean coral reefs, *Nature*, *450*(7166), 98–101, doi:10.1038/nature06252.

Orr, J. C., et al. (2005), Anthropogenic ocean acidification over the twenty-first century and its impact on calcifying organisms, *Nature*, *437*(7059), 681–686, doi:10.1038/nature04095.

Pan, Y., and R. T. Jackson (2008), Ethnic difference in the relationship between acute inflammation and serum ferritin in US adult males, *Epidemiol. Infect.*, *136*(03), 421–431, doi:10.1017/S095026880700831X.

Ragazzola, F., L. C. Foster, A. U. Form, J. Büscher, T. H. Hansteen, and J. Fietzke (2013), Phenotypic plasticity of coralline algae in a high CO2 world, *Ecol. Evol.*, *3*(10), 3436–3446, doi:10.1002/ece3.723.

Roff, G., C. Doropoulos, M. Zupan, A. Rogers, R. S. Steneck, Y. Golbuu, and P. J. Mumby (2015), Phase shift facilitation following cyclone disturbance on coral reefs, *Oecologia*, doi:10.1007/s00442-015-3282-x.

Shaw, E. C., S. R. Phinn, B. Tilbrook, and A. Steven (2014), Comparability of slack water and Lagrangian flow respirometry methods for community metabolic measurements, *PLoS One*, *9*(11), e112161, doi:10.1371/journal.pone.0112161.

Shaw, E. C., S. R. Phinn, B. Tilbrook, and A. Steven (2015), Natural in situ relationships suggest coral reef calcium carbonate production will decline with ocean acidification, *Limnol. Oceanogr.*, *60*(3), 777–788, doi:10.1002/lno.10048.

Silverman, J., D. I. Kline, L. Johnson, T. Rivlin, K. Schneider, J. Erez, B. Lazar, and K. Caldeira (2012), Carbon turnover rates in the One Tree Island reef: A 40-year perspective, *J. Geophys. Res.*, *117*, G03023, doi:10.1029/2012JG001974.

Smith, S. V. (1981), The Houtman Abrolhos Islands: Carbon metabolism of coral reefs at high latitude1, *Limnol. Oceanogr.*, *26*(4), 612–621, doi:10.4319/lo.1981.26.4.0612.

Suzuki, A., and H. Kawahata (2003), Carbon budget of coral reef systems: An overview of observations in fringing reefs, barrier reefs and atolls in the Indo-Pacific regions, *Tellus B*, *55*(2), 428–444, doi:10.1034/j.1600-0889.2003.01442.x.

Suzuki, A., H. Kawahata, T. Ayukai, and K. Goto (2001), The oceanic CO2 System and Carbon Budget in the Great Barrier Reef, Australia, *Geophys. Res. Lett.*, *28*, 1243–1246, doi:10.1029/2000GL011875.

Uppström, L. R. (1974), The boron/chlorinity ratio of deep-sea water from the Pacific Ocean, *Deep Sea Res. Oceanogr. Abstr.*, *21*(2), 161–162, doi:10.1016/0011-7471(74)90074-6.

Watanabe, A., H. Kayanne, H. Hata, S. Kudo, K. Nozaki, K. Kato, A. Negishi, Y. Ikeda, and H. Yamano (2006), Analysis of the seawater CO2 system in the barrier reef-lagoon system of Palau using total alkalinity-dissolved inorganic carbon diagrams, *Limnol. Oceanogr.*, *51*(4), 1614–1628, doi:10.4319/lo.2006.51.4.1614.

Zhang, Z., J. Falter, R. Lowe, and G. Ivey (2012), The combined influence of hydrodynamic forcing and calcification on the spatial distribution of alkalinity in a coral reef system, *J. Geophys. Res.*, *117*(C4), doi:10.1029/2011JC007603.